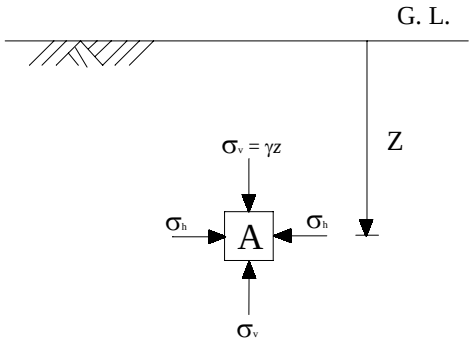

(a)

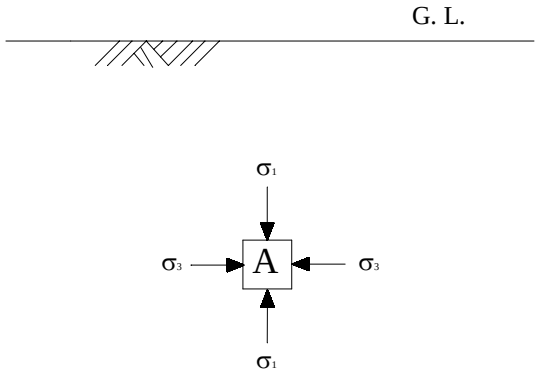

(b)

Fig. 2.1 Development of in-situ stresses

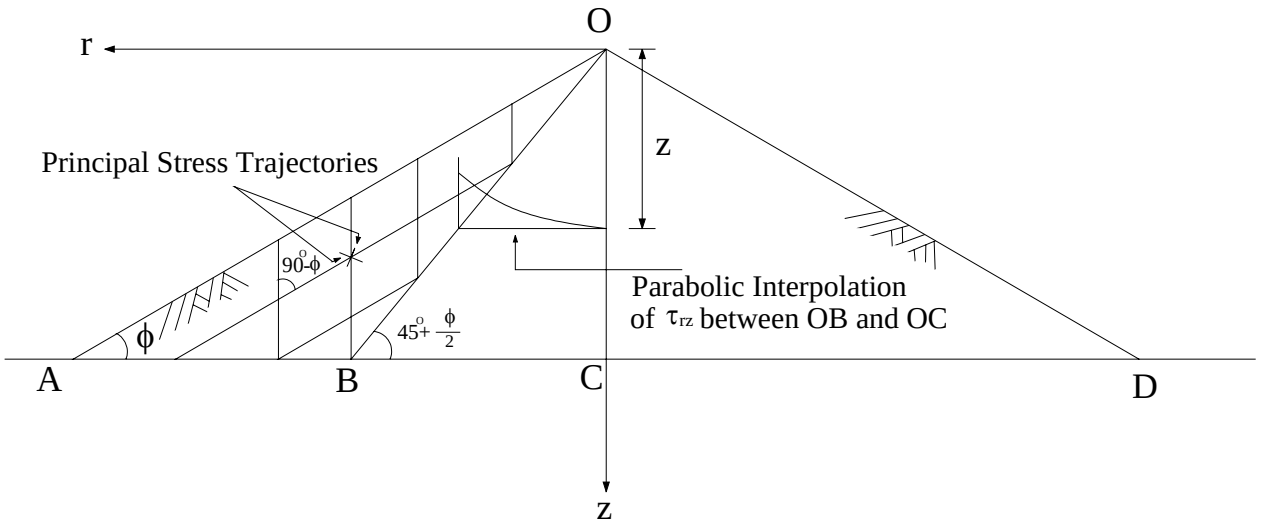

Fig. 2.2. Jaky's formulation of the relationship between K_o on OC and ϕ mobilized in OAB (after Mesri and Hayat, 1993)

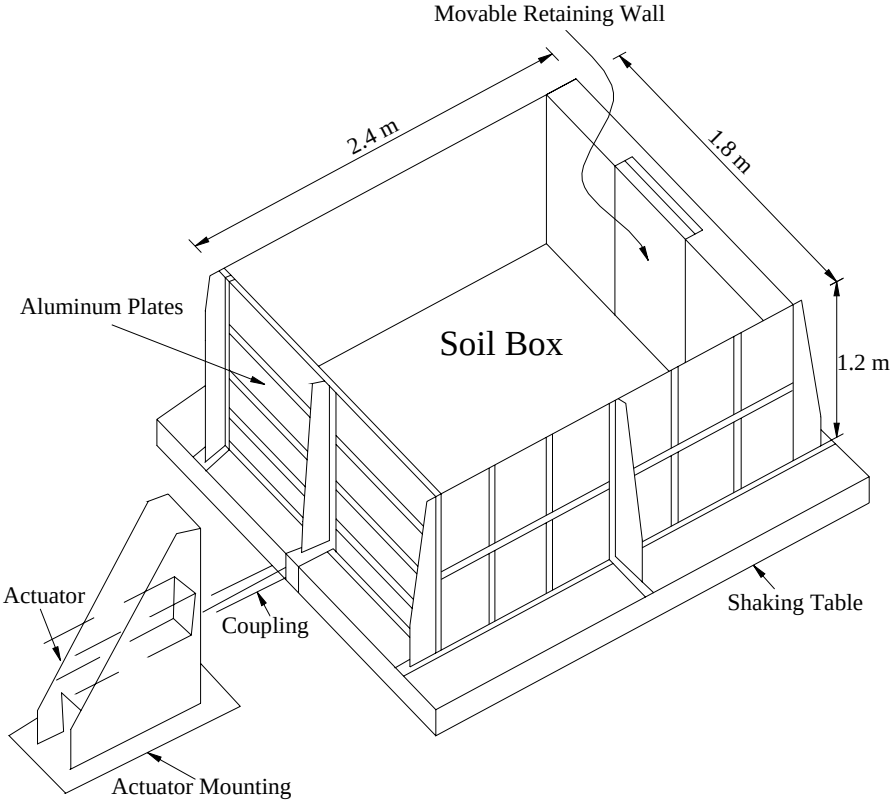

Fig. 2.3. Shaking table, soil box, and actuator
(after Sherif et al., 1981)

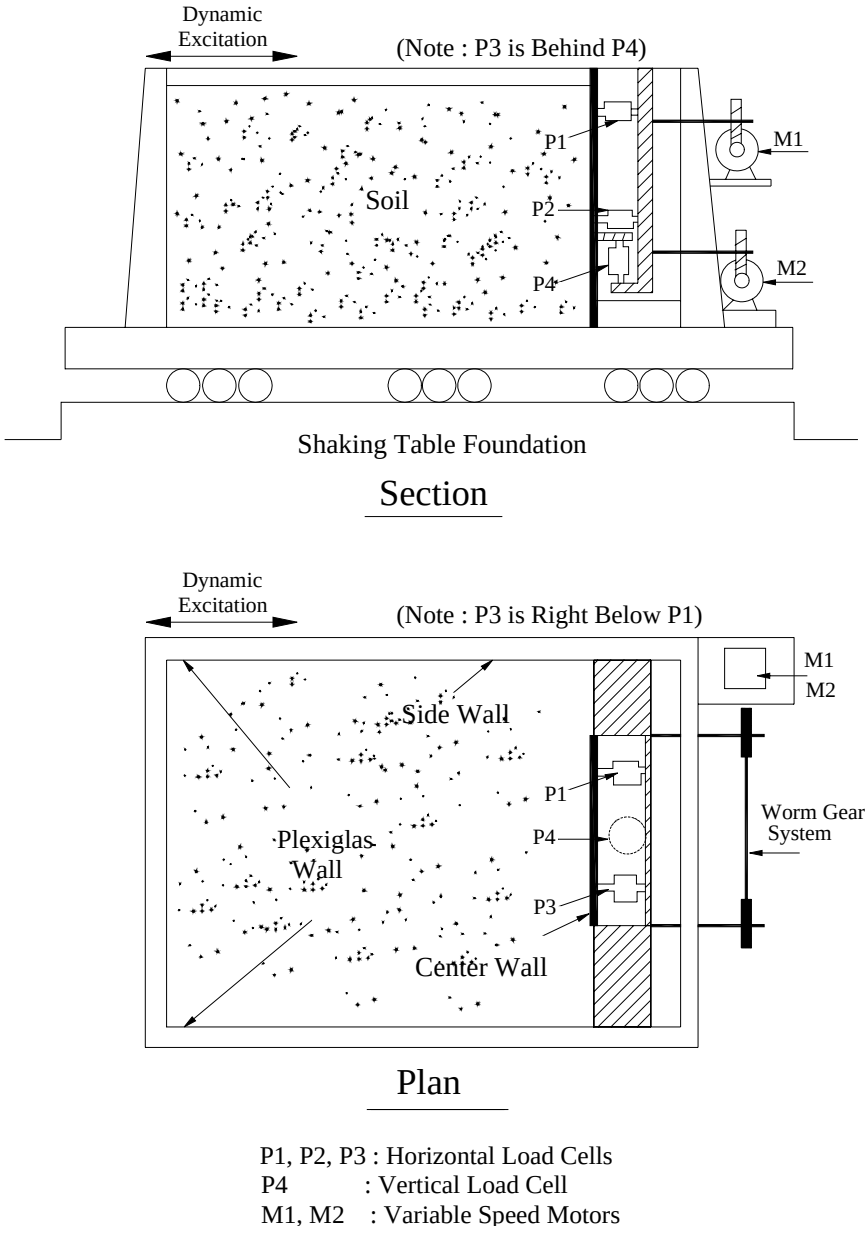

Fig. 2.4. Shaking table with movable retaining wall
(after Sherif et al., 1984)

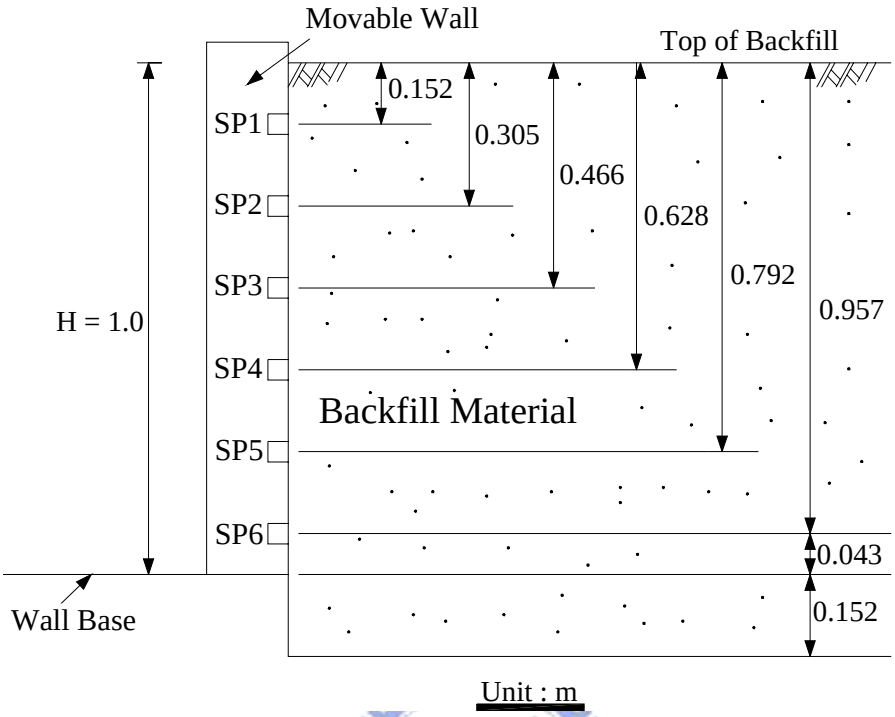

Fig. 2.5. Locations of soil-pressure transducers (after Sherif et al., 1984)

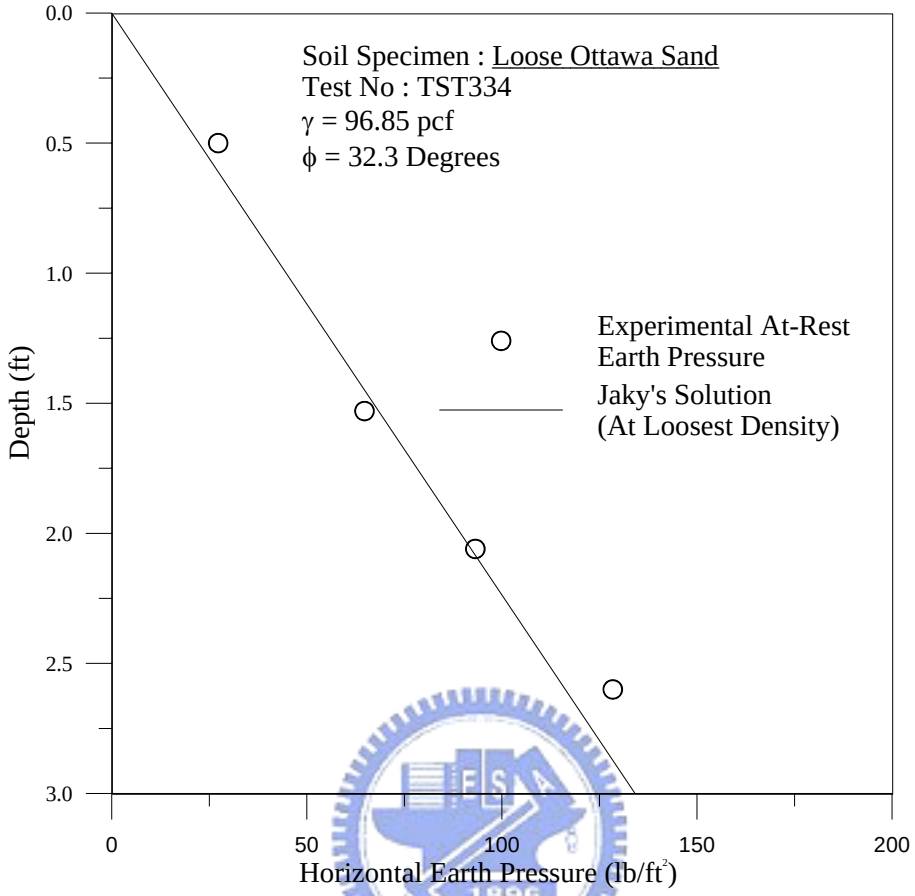

Fig. 2.6. Distribution of at-rest stresses for loose sand (after Sherif et al., 1984)

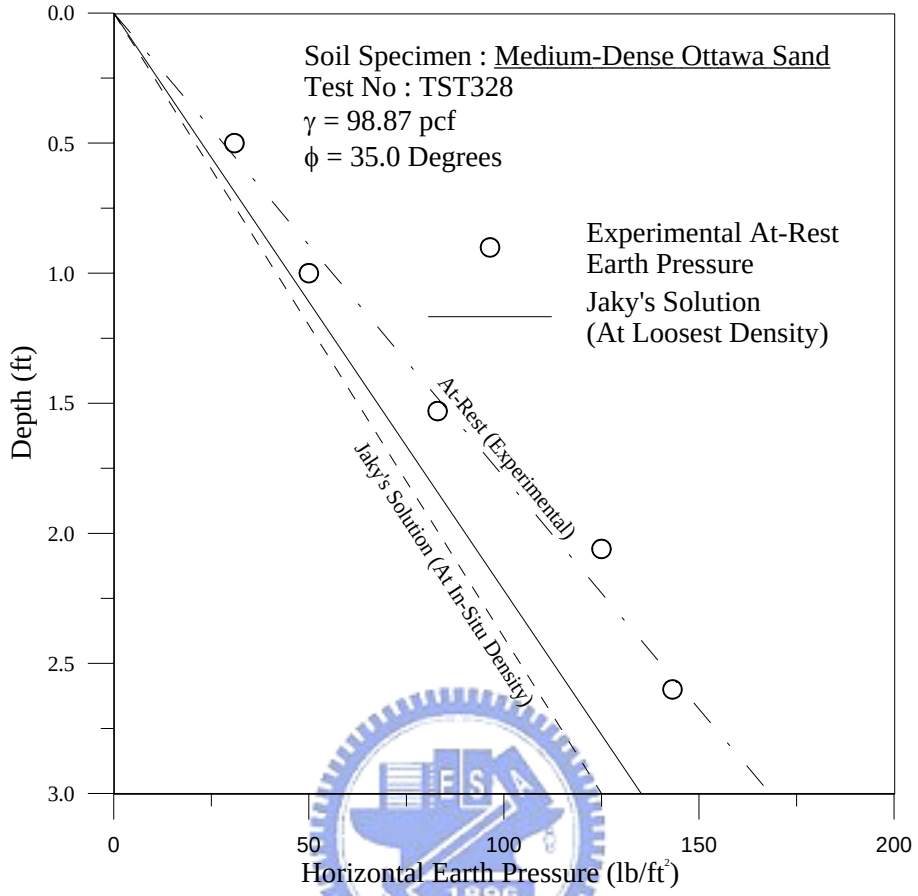

Fig. 2.7. Distribution of at-rest stresses for medium-dense sand (after Sherif et al., 1984)

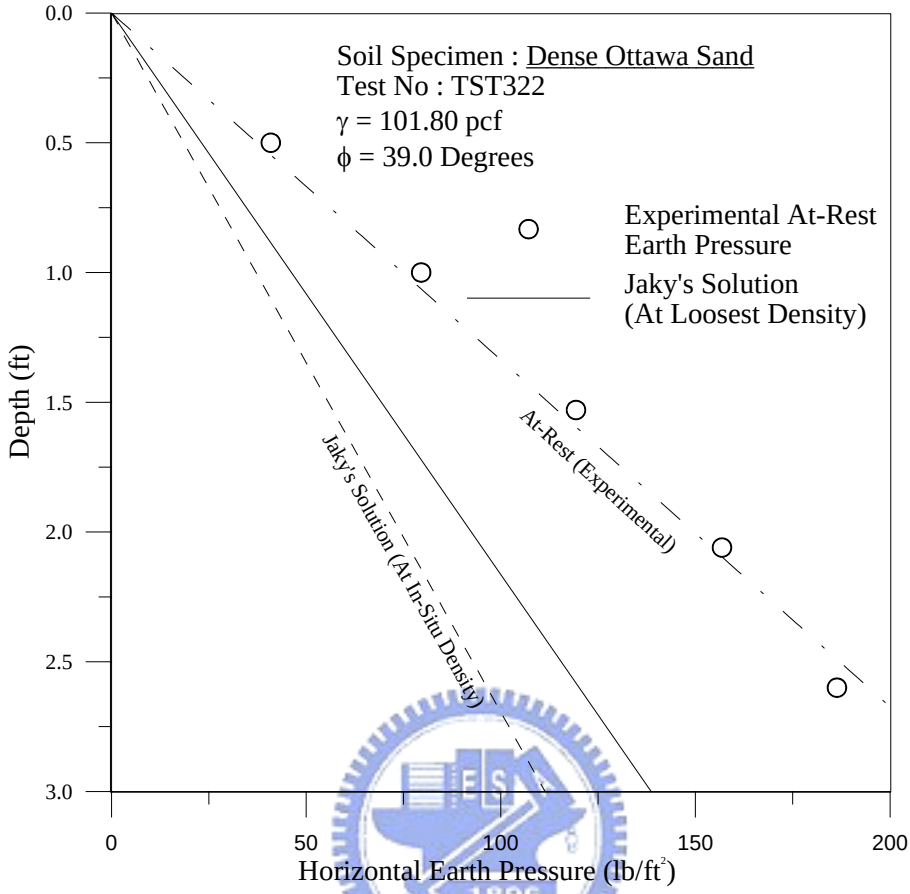

Fig. 2.8. Distribution of at-rest stresses for dense sand (after Sherif et al., 1984)

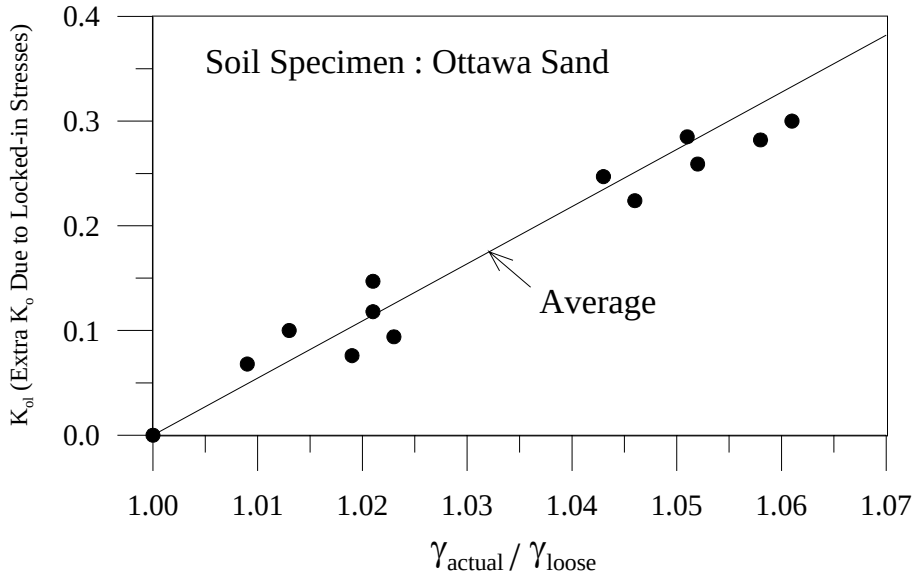

Fig. 2.9. Lock-in at-rest pressure due to soil densification (after Sherif et al., 1984)

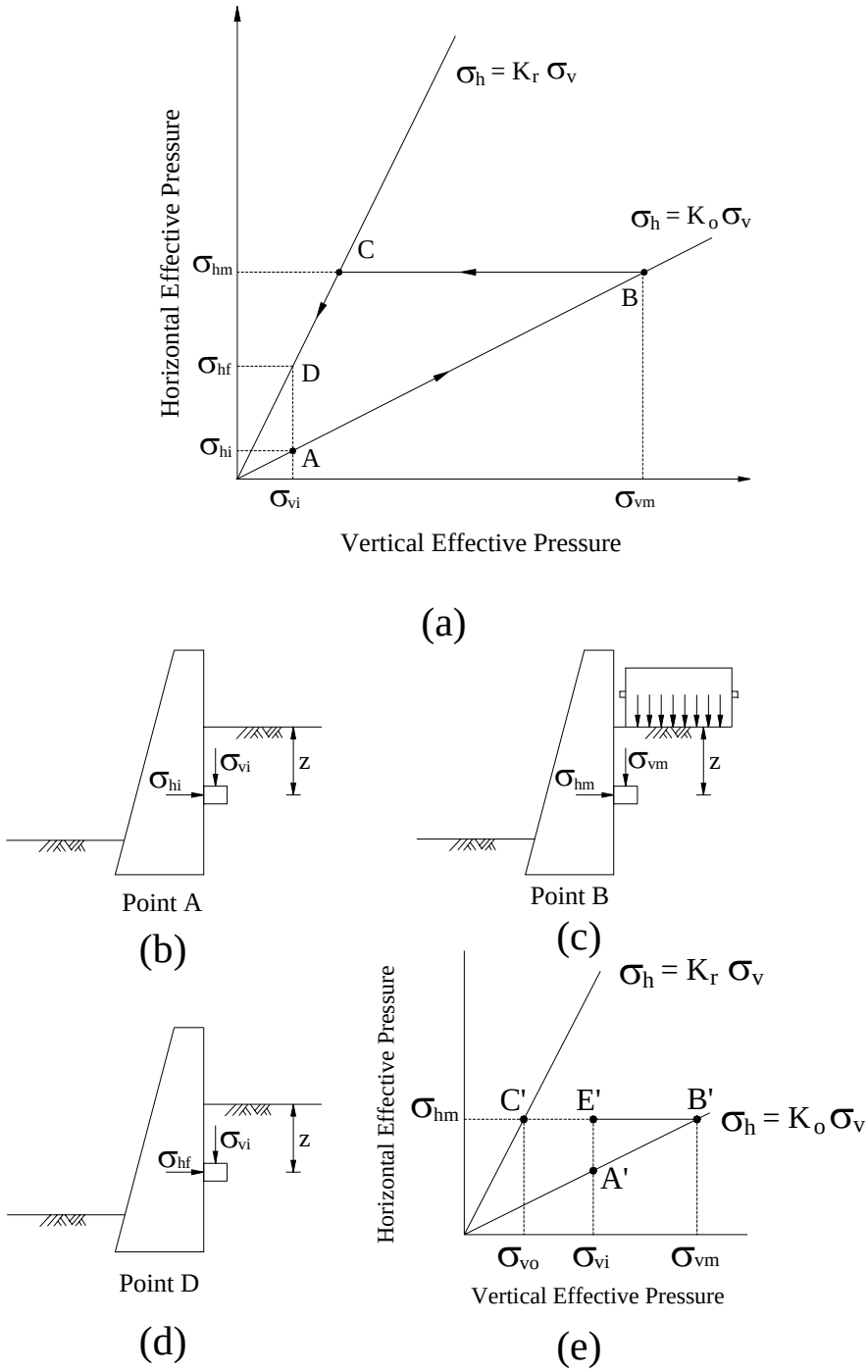

Fig. 2.10. Broms's simplified compaction pressure theory (after Broms, 1971)

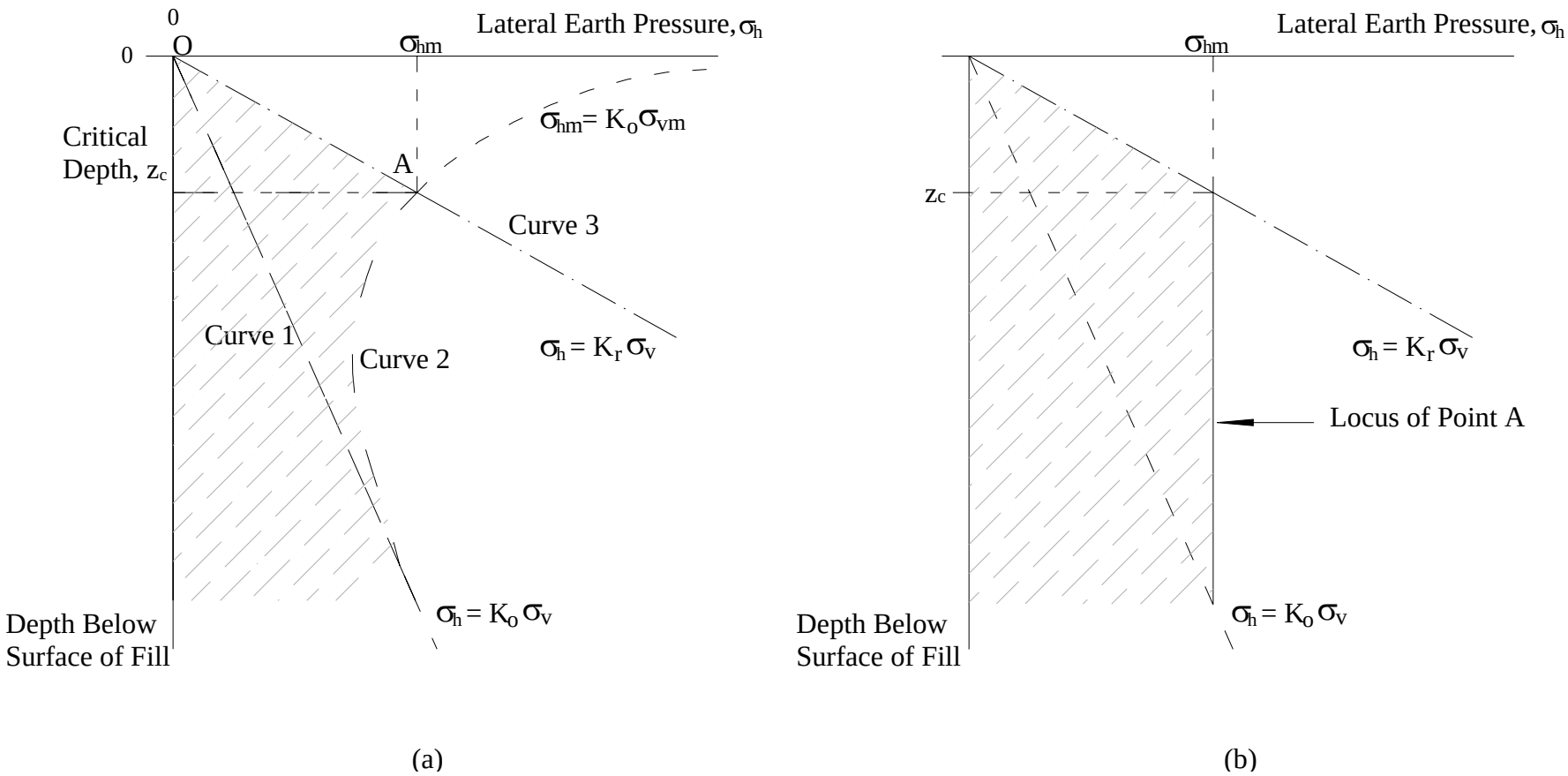

Fig. 2.11. Lateral pressure distribution due to compaction of fill (after Broms, 1971)

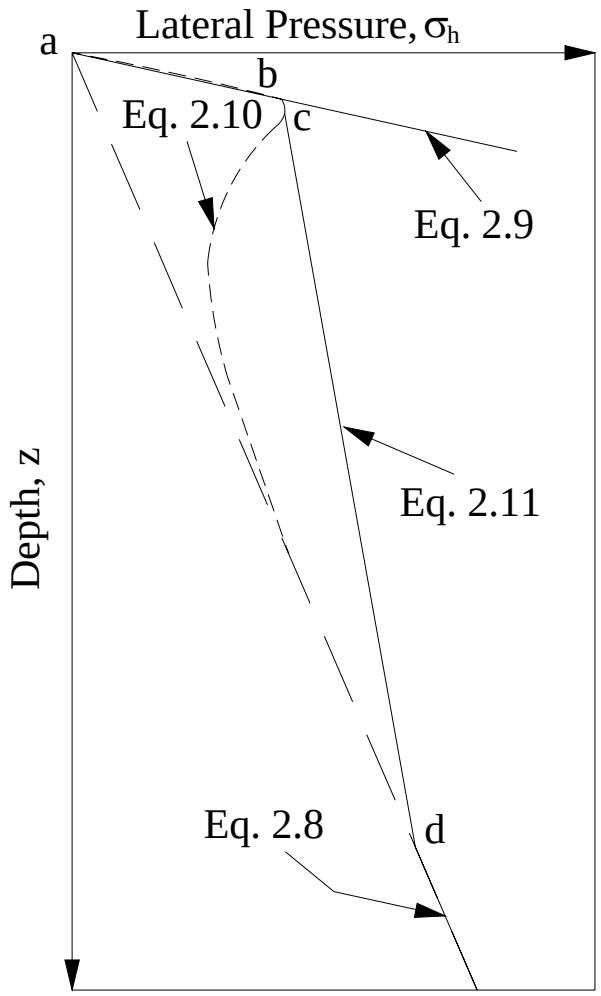

Fig. 2.12. Hand-calculation for estimating σ_h
(after Peck and Mesri, 1987)

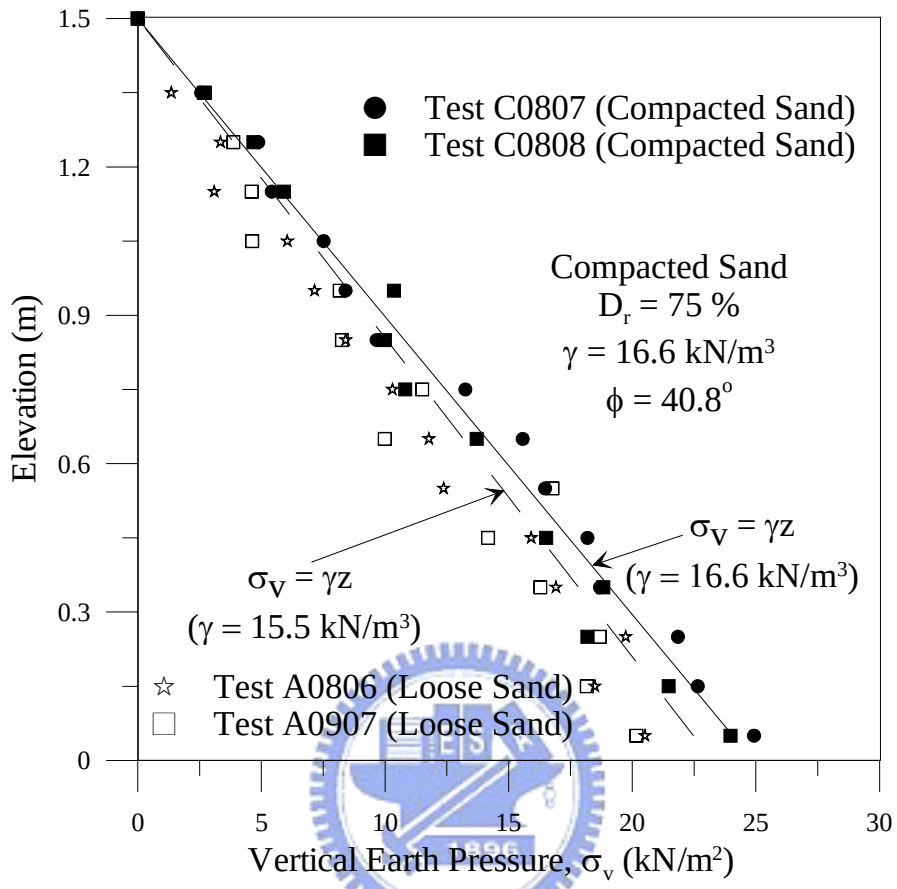

Fig. 2.13. Distribution of vertical earth pressure measured in soil mass (after Chen, 2002)

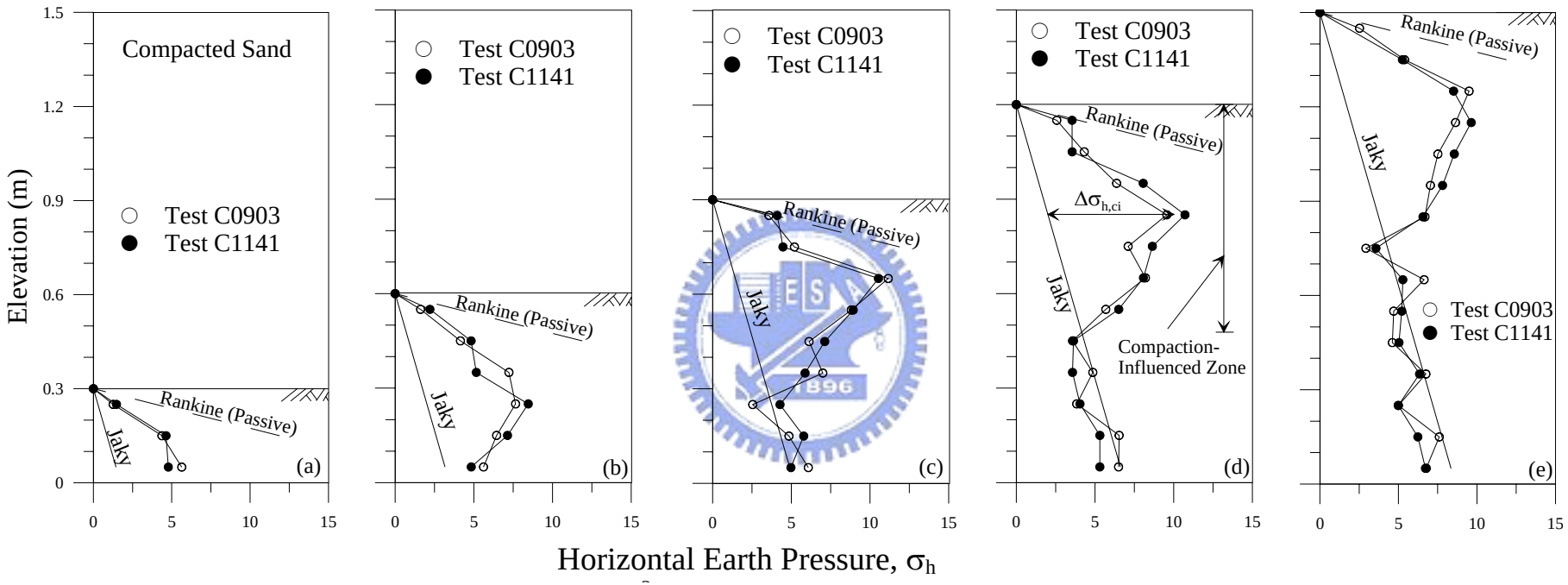

Fig. 2.14. Distribution of horizontal earth pressure after compaction
(after Chen, 2002)

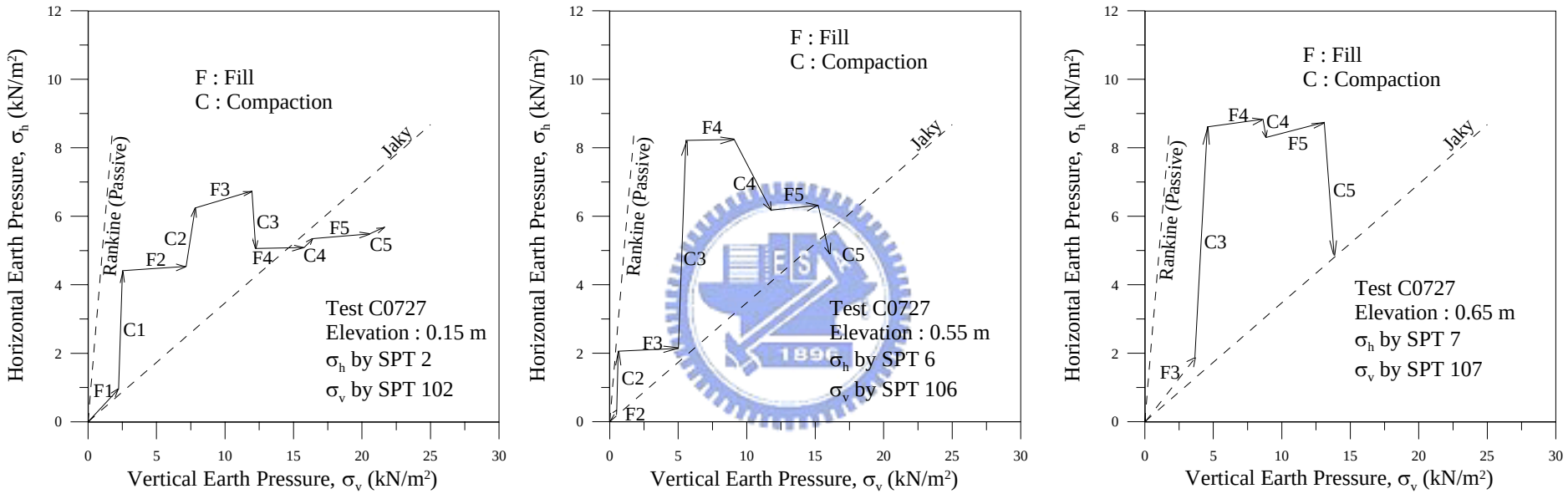

(a) (b) (c)

Fig. 2.15. Stress path of a soil element under compaction
(after Chen, 2002)

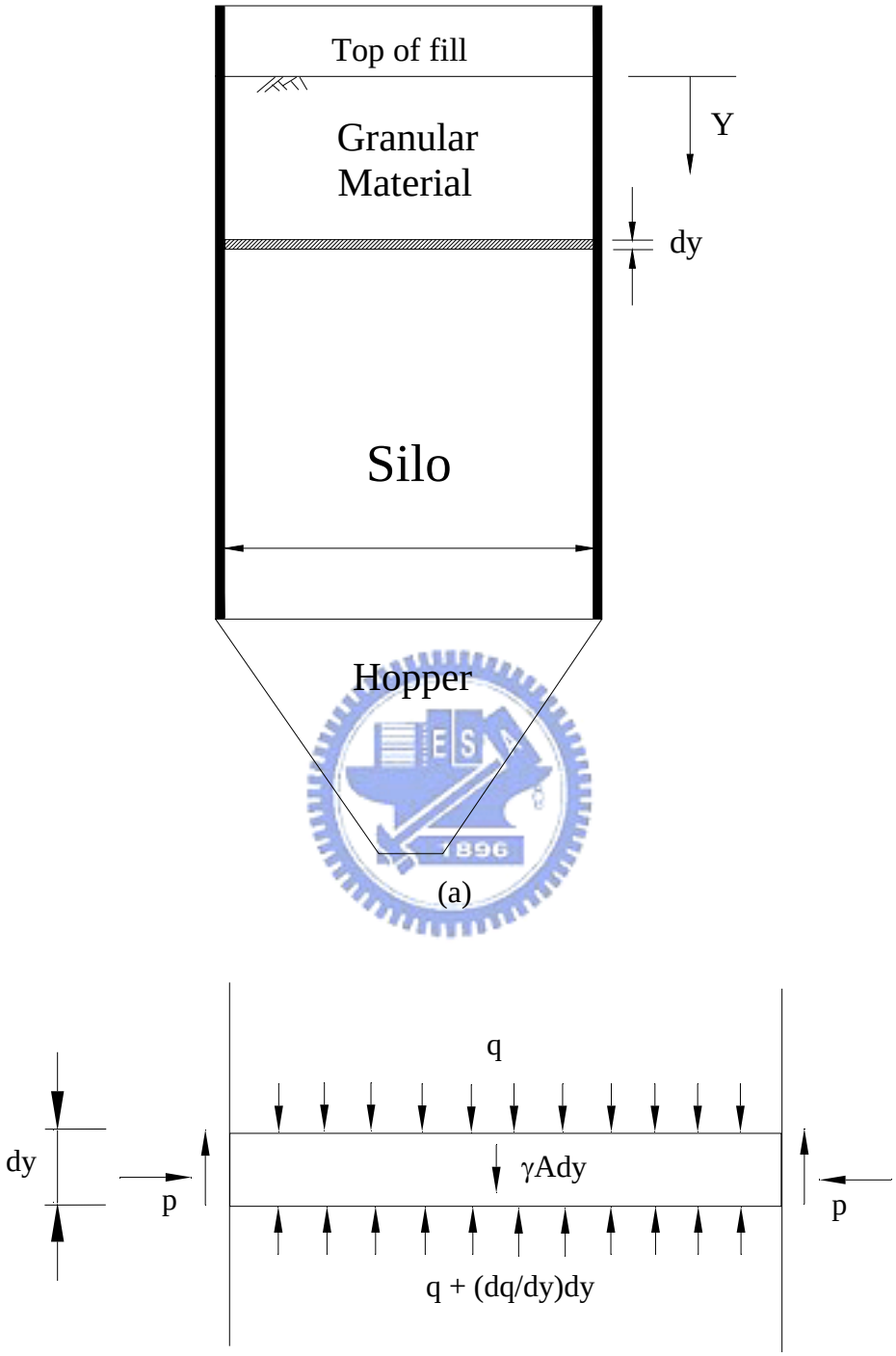

Fig. 2.16. Horizontal lamina for derivation of Janssen's equations (redrawn after Safarian and Harris, 1985)

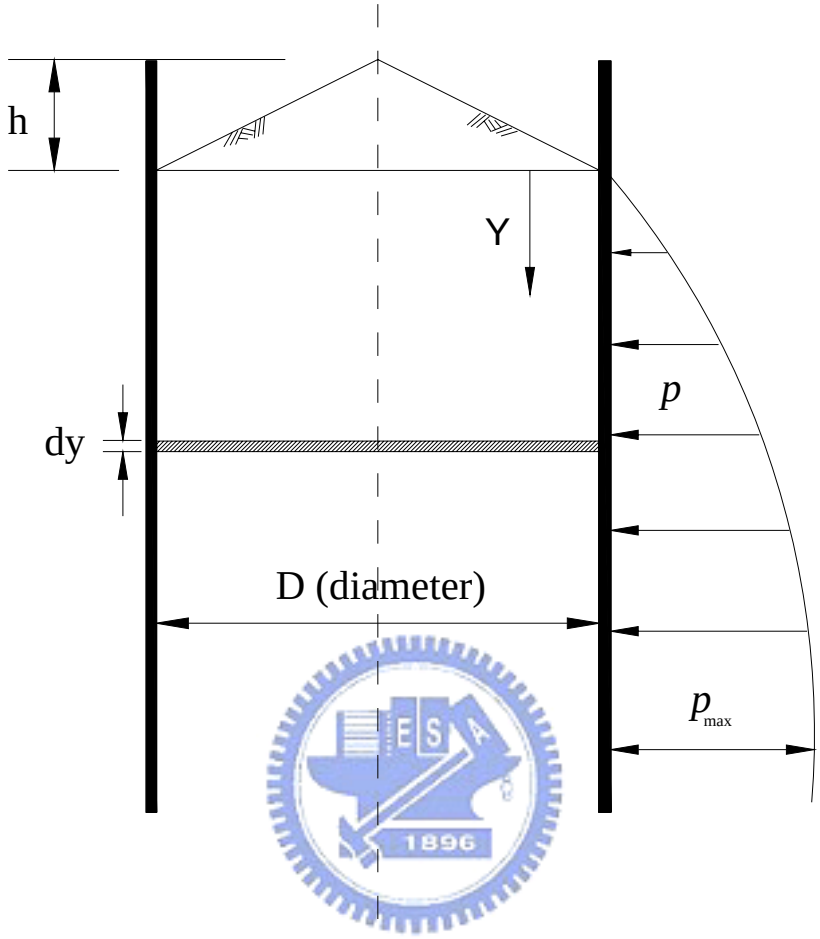

(a)

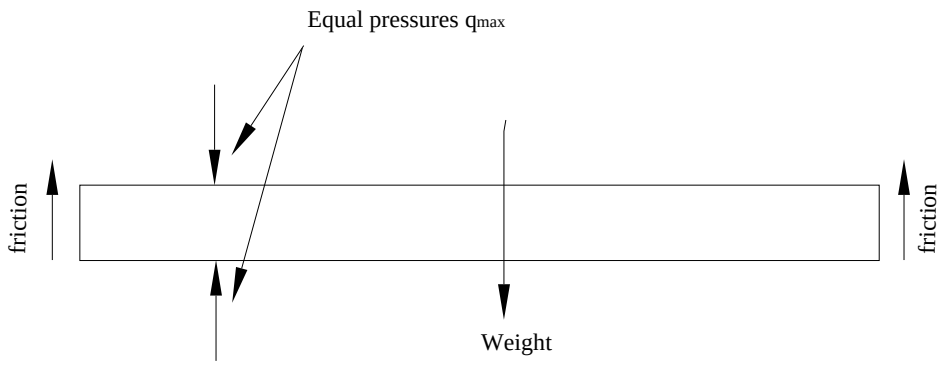

(b)

Fig. 2.17. Lamina of stored material for derivation of the Reimbert's equations (after Reimbert and Reimbert, 1895)

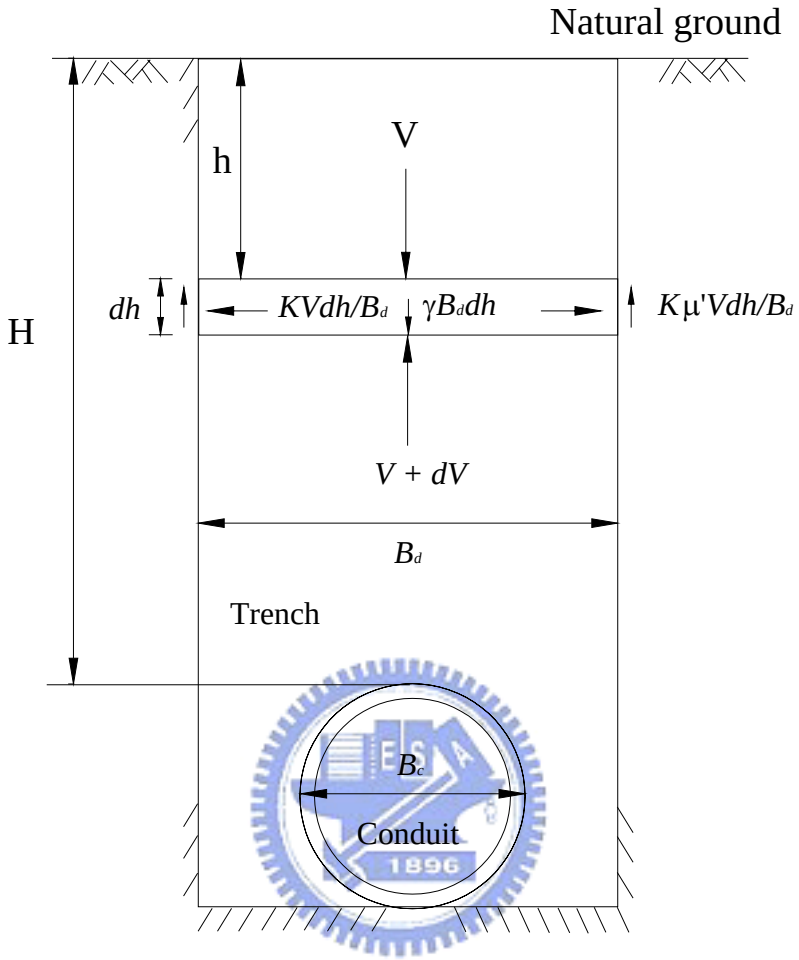

Fig. 2.18. Free-body diagram for ditch conduit
(after Spangler and Handy, 1984)

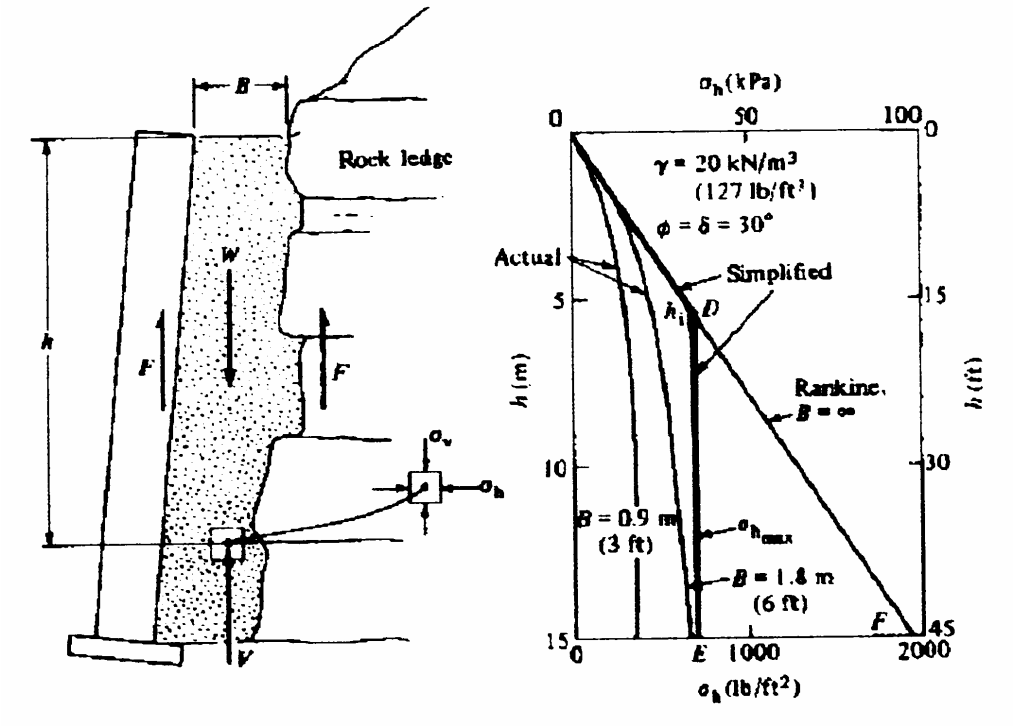

(a) (b)

Fig. 2.19. Distribution of soil pressure against fascia walls to partial support from wall friction F (after Spangler and Handy, 1984)

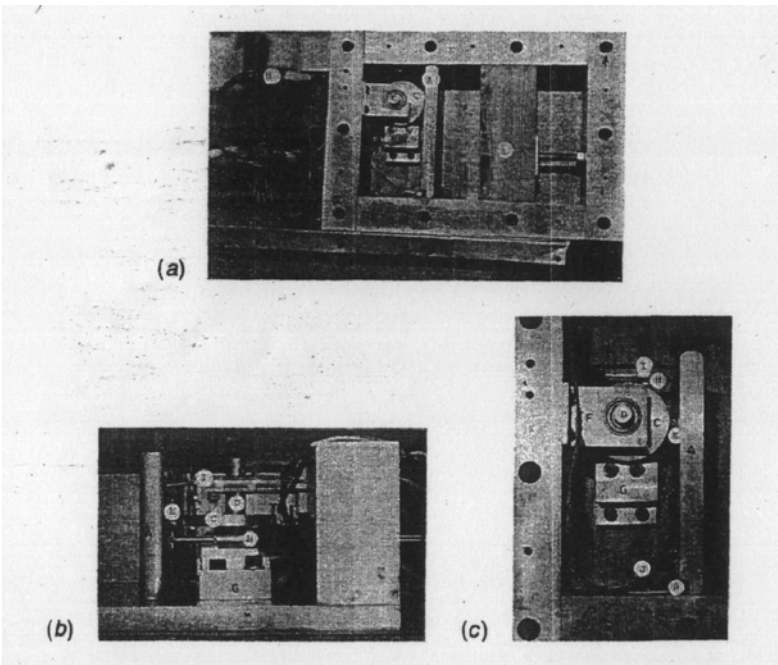

(a)

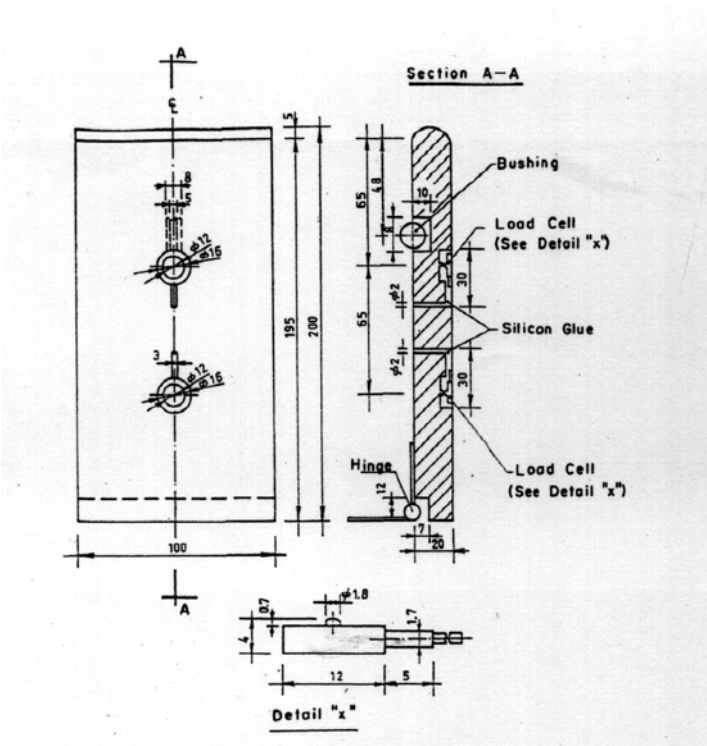

(b)

Fig. 2.20. Model retaining wall (after Frydman and Keissar, 1987)